AJNR

Effective Dose Measurements of the Latest-Generation Angiographic System in Patients with Acute Stroke: A Comparison with the Newest Multidetector CT Generation

A. Brehm, K.A.T. Nguyen, K.A. Blackham and M.-N. Psychogios

AJNR Am J Neuroradiol published online 6 October 2022
http://www.ajnr.org/content/early/2022/10/06/ajnr.A7658

Published October 6, 2022 as 10.3174/ajnr.A7658

Effective Dose Measurements of the Latest-Generation Angiographic System in Patients with Acute Stroke: A Comparison with the Newest Multidetector CT Generation

A. Brehm, K.A.T. Nguyen, K.A. Blackham, and M.-N. Psychogios

ABSTRACT

BACKGROUND AND PURPOSE: Patients with acute ischemic stroke are increasingly triaged with one-stop management approaches, resulting in baseline imaging with a flat detector CT scanner. This study aimed to estimate the effective dose to a patient of a novel cervical and intracranial flat detector CT angiography and a flat detector CT perfusion protocol and to compare it with the effective dose of analogous multidetector row CT protocols.

MATERIALS AND METHODS: We estimated the effective dose to the patient according to the International Commission on Radiological Protection 103 using an anthropomorphic phantom with metal oxide semiconductor field effect transistor dosimeters. Placement was according to the organ map provided by the phantom manufacturer. We used 100 measurement points within the phantom, and 18 metal oxide semiconductor field effect transistor dosimeters were placed on the surface of the phantom. All protocols followed the manufacturer's specifications, and patient positioning and collimation were performed as in routine clinical practice. Measurements were obtained on the latest-generation angiography and multidetector row CT systems with identical placement of the metal oxide semiconductor field effect transistor dosimeters.

RESULTS: The estimated effective doses of the investigated perfusion protocols were 4.52 mSv (flat detector CT perfusion without collimation), 2.88 mSv (flat detector CT perfusion with collimation), and 2.17 mSv (multidetector row CT perfusion). A novel protocol called portrait flat detector CT angiography that has a z-axis coverage area comparable with that of multidetector row CT angiography had an estimated effective dose of 0.91 mSv, while the dose from multidetector row CT was 1.35 mSv.

CONCLUSIONS: The estimated effective dose to the patient for flat detector CT perfusion and angiography on a modern biplane angiography system does not deviate substantially from that of analogous multidetector row CT protocols.

ABBREVIATIONS: AIS = acute ischemic stroke; FDCT = flat detector CT; FDCT-A = flat detector CT angiography; FDCT-P = flat detector CT perfusion; ICRP = International Commission on Radiologic Protection; MDCT = multidetector CT; MDCT-A = multidetector CT angiography; MDCT-P = multidetector CT perfusion; MOSFET = metal oxide semiconductor field effect transistor

Implementing a one-stop management workflow can substantially shorten door-to-groin and door-to-reperfusion times.[1,2] It can, furthermore, lead to improved patient outcomes according to a recently published randomized controlled trial.[3] The one-stop management workflow combines diagnostic imaging and interventional therapy of patients with acute ischemic stroke (AIS) in 1 room—the angiography suite. Flat detector CT (FDCT) is used for the initial diagnostic imaging rather than the traditional approach in which the patient must first be transported to the multidetector CT (MDCT) room for diagnostic imaging and then subsequently to the angiography suite for treatment.[1] One possible disadvantage of FDCT compared with MDCT is the limited coverage of FDCT angiography (FDCT-A), because it is impossible to simultaneously visualize the intracranial vessels, the extracranial vessels. and the aortic arch. This limitation was recently partially resolved by the introduction of a new portrait FDCT-A prototype in which the detector is rotated by 90° for an increased FOV. Furthermore, a recent publication showed a strong correlation between FDCT-perfusion (FDCT-P) and multidetector row perfusion (MDCT-P) for the automated measurements of ischemic core and ischemic penumbra volumes in patients with AIS, suggesting that FDCT-P can be used as effectively and reliably as MDCT-P.[4] Despite the growing use of these protocols, the effective dose to the patient and, more specifically, the dose to the lens of the eye were not systematically compared with analogous MDCT protocols.

Received March 22, 2022; accepted after revision August 6.

From the Department of Neuroradiology, Clinic of Radiology and Nuclear Medicine, University Hospital Basel, Basel, Switzerland.

Please address correspondence to Alex Brehm, PhD, Department of Neuroradiology, Clinic of Radiology and Nuclear Medicine, University Hospital Basel, Petersgraben 4, 4031 Basel, Switzerland; e-mail: alex.brehm@usb.ch

http://dx.doi.org/10.3174/ajnr.A7658

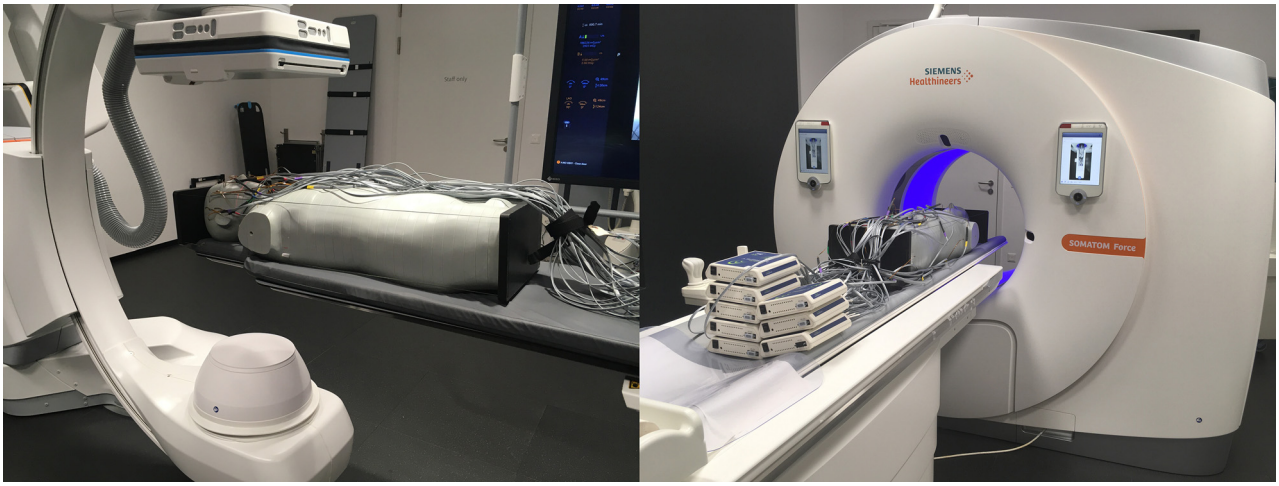

FIG 1. The anthropomorphic ATOM phantom used for effective dose measurement. The phantom in an experimental setup for 3D acquisition is equipped with MOSFET dosimeters on an Artis icono biplane angiography system (*left*) and on the Somatom Force CT scanner (*right*).

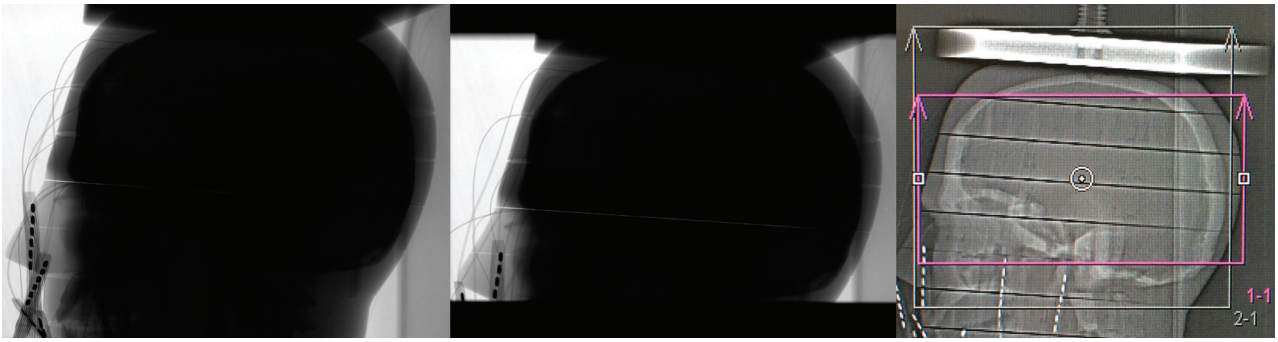

FIG 2. Lateral view of the investigated head area of the phantom for uncollimated measurement (*left*) and collimated measurement (*middle*) of the 60s DCT head perfusion protocol on the Artis icono and for perfusion measurement on the Somatom Force (*right*).

In the present study, we used a phantom to measure the effective dose to the patient and the eye lens dose of FDCT-P and portrait FDCT-A and to compare the results obtained with those obtained from analogous MDCT protocols.

MATERIALS AND METHODS

Phantom

We used an adult male ATOM phantom 701-C (Computerized Imaging Reference Systems) to measure the effective dose (Fig 1); the phantom represents the body of a male human with a height of 173 cm and a body weight of 73 kg. The phantom consists of averaged materials for soft, bone, lung, and brain tissues. The phantom is equipped with 39 slices of 2.5-cm thickness, all of them having cavities for detector placement in a 1.5 × 1.5 cm grid with a 0.5-cm diameter.

Dosimeters

For assessing the organ dose, we used metal oxide semiconductor field effect transistor (MOSFET) TN 1002RD-H dosimeters used with the MobileMOSFET system, model TN-RD-70-W (Best Medical Canada). The MobileMOSFET system consists of a remote monitoring dose-verification software, a Bluetooth wireless transceiver, and a reader module that acts as a channel between the MOSFET dosimeters and software. Up to 5 MOSFET dosimeters can be connected to 1 reader. In this study, 8 readers and 40 MOSFET dosimeters were used for simultaneous measurements. Before the measurements, all MOSFET dosimeters were calibrated. For calibration purposes, each of the MOSFET dosimeters was irradiated with a specified dose. The dose was then measured with an ionization chamber (PM500-CII 52.8210; Capintec) connected to the Unidos dosimeter (PTW Frieburg) as described before.[5]

C-Arm Angiography and CT Systems

We performed the measurements on an Artis icono biplane angiography system (Siemens Healthineers AG) with a Neuro Tabletop and Mattress (https://www.sgmattress.sg/) and on a Somatom Force CT scanner (Siemens Healthineers AG) with syngo CT VB20 software. For measurements on the Artis icono system, the A-plane C-arm was placed in the anterior-posterior position and the FOV for 3D imaging was set in the head region of the phantom. The perfusion measurements on the Artis icono system were performed with and without collimation of the x-ray field (Fig 2). The craniocaudal collimation and positioning of the phantom was applied according to the procedure-specific settings used in the clinical workflow at

the University Hospital Basel. The scan z-coverage in the collimated setup was 15 cm, derived from averaging the scan z-coverage of all scans obtained at the University Hospital Basel. The protocol is described in detail elsewhere.[6] For perfusion measurements on the Somatom Force CT scanner, we used the standard acquisition protocol from the manufacturer. The scan z-coverage for perfusion measurements on the Somatom Force system is 11.4 cm.

In addition, we investigated the 3D imaging protocols for visualization of the carotid and intracranial arteries. The acquisition protocols for both systems were used as in clinical practice. For measurements on the Artis icono system, the detector was used in portrait mode without collimation (Fig 3). The imaging protocol with the detector in portrait mode (ie, rotated by 90°) is the latest 3D imaging prototype on the Artis icono. For 3D imaging of the carotid arteries on the Somatom Force CT scanner, the CARE Dose 4D and CARE kV technologies (Siemens) were applied. To ensure comparable results, we used the same z-coverage area for the FDCT-A and MDCT angiography (MDCT-A), excluding the aortic arch. We summarized the technical parameters of the 3D acquisition protocols for both systems in Tables 1 and 2.

Estimation of Effective Dose

To estimate the organ dose, we placed the MOSFET dosimeters in 118 measurement points in the ATOM phantom and on the phantom surface. The locations of the measurement points within the phantom were defined according to the organ map provided by the phantom manufacturer. These locations represent the anatomic positions of different organs (brain, eye lenses, salivary glands, thyroid, esophagus, bone surface, lung, liver, stomach, pancreas, adrenal gland, small intestine, spleen, kidney, red bone marrow, bladder, gonads, and so forth). To fit the MOSFET dosimeters within the phantom holes, we placed each dosimeter into the tissue-equivalent holder. The skin dose was measured by 18 dosimeters positioned on the surface of the phantom at slices 4, 10, 17, 28, and 38. We used

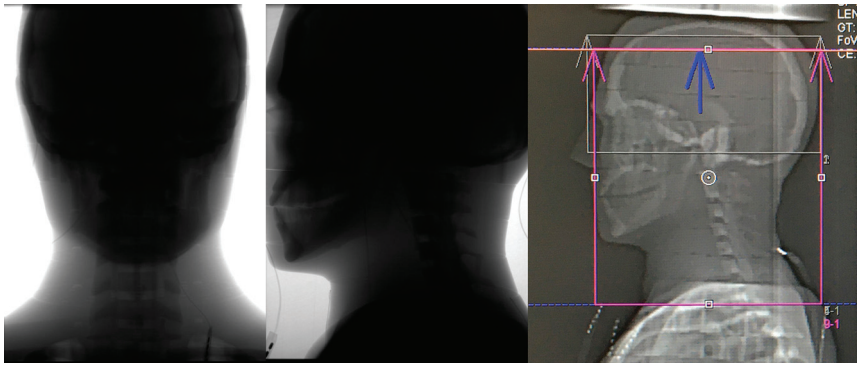

FIG 3. The position of the investigated head area of the phantom for carotid measurement on the Artis icono in frontal (*left*) and lateral (*middle*) views and on the Somatom Force in the lateral view (*right*).

Table 1: Technical parameters of investigated 3D imaging protocols (brain perfusion, portrait angiography with head and neck angiography), measured eye lens dose (for left, right eye and mean), and effective dose for the anthropomorphic ATOM male phantom on Artis icono

3D Imaging Protocol Parameters	60s DCT Head Perfusion (10 Rotations)		4s DCT Head Portrait (1 Rotation)
Reconstructed volume size (diameter × height) (cm)	24 × 18.5 (uncollimated)	24 × 15[a]	18.5 × 24 (uncollimated)
Tube voltage (nominal) (kV)	70	70	90
Dose/frame (nominal) (nGy/f)	360	360	1200
Rotation range	200°	200°	200°
Angulation step (*df*)	0.8	0.8	0.8
Eye lens dose (mean) (mGY)	65 and 69 (SD, 67)	54 and 58 (SD, 56)	7.7 and 8.3 (SD, 8)
Estimated effective dose (mSv)	4.52	2.88	0.91

Note:—60s DCT indicates 60s Dyna-CT; 4s DCT, 4s Dyna CT.
[a] Collimation was defined on the basis of usual clinical workflow at the University Hospital Basel.

Table 2: Technical parameters of investigated protocols (brain perfusion and head and neck angiography), measured eye lens dose (for left, right eye and mean), and effective dose for the anthropomorphic ATOM male phantom on Somatom Force

3D Imaging Protocol Parameters	NeuroVPCT_Prolonged, DynMulti4D	NeuroVPCT_Prolonged, Head Angio
Scan coverage (cm)	11.4	24
Tube voltage (kV)	70	90
Scan duration (sec)	60	NA
Number of cycles @ 1.5 seconds cycle time	30	NA
CTDIvol (mGy)	144.2	19,9
DLP (mGy × cm)	2169.5	550
Eye lens dose (mean) (mGy)	119 and 125 (SD, 122)	11.8 and 11.7 (SD, 11.8)
Estimated effective dose (mSv)	2.17	1.35

Note:—CTDIvol indicates volume CT dose index; DLP, dose-length product; NA, not applicable.

Table 3: Organ dose in milligrays for selected organs and tissues of investigated 3D imaging protocols on the Artis icono

Organ	60s DCT Head Perfusion (10 Rotations, Uncollimated)	60s DCT Head Perfusion (10 Rotations, Collimated)	4s DCT Head Portrait (1 Rotation)
Brain	100.8	84.7	11.8
Salivary glands	56.2	7.4	11.4
Thyroid	3.5	1.8	6.1
Lung	1.3	0.8	0.2
Red bone marrow	17.4	12.1	2.4
Esophagus	1.1	0.7	0.8

Table 4: Organ dose in milligrays for selected organs and tissues of investigated 3D imaging protocols on the Somatom force

Organ	NeuroVPCT_Prolonged, DynMulti4D	NeuroVPCT_Prolonged, Head Angio
Brain	71.6	7.8
Salivary glands	6.4	8
Thyroid	1.3	17.2
Lung	0.4	1.3
Red bone marrow	9.2	1.3
Esophagus	0.4	2.0

the same distribution and positioning of the dosimeters in all measurements.

With the identical setup of dosimeters, we repeated all 3D imaging protocols 3 times to ensure adequate radiation of the dosimeters outside the direct radiation field. The organ dose was calculated as the mean value of the measured data from all dosimeters placed into the respective organ sites. For organs such as skin, red bone marrow, esophagus, and lungs that. depending on the applied 3D imaging protocol and the scanned area, were exposed to both direct and scattered radiation, the fraction of directly irradiated organ volume in the head and neck region was considered for calculation of the organ dose. The fraction of the directly irradiated skin area was estimated according to the so-called "rule of nines" used in trauma and emergency medicine to assess the total body surface area involved in patients with burns.[7] We estimated it to be 8% for the whole-head region and 10% for the head and neck region. The red bone marrow in the whole-head region was considered to be roughly 10%, and in the head and neck region, it was roughly 15% of total body red marrow.[8] These data were used to calculate the effective dose according to the guidelines of the International Commission on Radiologic Protection (ICRP) 103.[9] The radiation-weighting factor for x-ray was assumed to be 1 in concordance with the ICRP 103.[9]

The accuracy of our measurements was estimated to be ±20%. This estimation considers all possible sources of errors, such as uncertainty of the reference dosimeter, uncertainty of estimation of calibration factors, and the uncertainty of calculation of the dose for each organ location.

RESULTS

We summarized the estimated effective dose to the patient values for the investigated FDCT protocols in Table 1 and the investigated MDCT protocols in Table 2.

The estimated effective dose to a patient of the FDCT-P protocol was 4.52 mSv without collimation and 2.88 mSv with collimation. The collimated dose of FDCT-P was 33% higher than the measured dose on MDCT (2.17 mSv). Eye lens doses of the perfusion protocols were 2-fold higher on MDCT (122 mGy) compared with uncollimated FDCT (67 mGy) and collimated FDCT (56 mGy).

The estimated effective dose to a patient of the portrait FDCT-A (0.91 mSv) was 48% lower than the effective dose of the corresponding MDCT-A protocol (1.35 mSv). The eye lens dose was also lower at 8 mGy compared with 11.8 mGy.

In all measurements, at least 95% of the radiation was recorded in the brain, red bone marrow, salivary glands, lung, esophagus, and thyroid. The remaining organs received <5% of the radiation, rendering them relatively clinically unimportant. A detailed overview of the dose distribution can be found in the Tables 3 and 4.

DISCUSSION

Our study has the following main findings: 1) Collimation has a powerful impact on the estimated effective dose to the patient because it can reduce the dose by almost 50%, 2) the estimated effective dose to the patient of the collimated FDCT-P and of the portrait FDCT-A does not deviate substantially from analogous MDCT protocols, and 3) the eye lens dose appears to be similar on FDCT and MDCT.

Two prior publications estimating the effective dose to a patient of FDCT-P on predecessor systems (Artis Q and Artis Axiom; Siemens Healthineers AG) reported higher doses with 5.9 and 5.1 mSv, respectively.[6,10] However, these measurements must be compared with our uncollimated dose results (4.52 mSv) because no use of collimation was reported in either publication. In this case, a 12% difference in the measurements of Struffert et al[13] is well within the margin of error; however, the 30% difference compared with our prior publication[6] is outside this margin. This difference could partly be explained by a different phantom and fewer measurement points. Furthermore, the directly and indirectly irradiated tissues were not analyzed separately in our previous publication, possibly leading to an overestimation of the organ doses, especially red bone marrow.[8] From a clinical standpoint, the collimated dose of FDCT-P is more important because the z-coverage can easily be reduced to parallel the parameters of MDCT-P.

Even more relevant is our result that the effective dose estimated for the collimated FDCT-P is only slightly higher than that with MDCT-P (33%), despite the considerably larger z-axis coverage area of 15 cm compared with the MDCT-P coverage of 11.4 cm (Fig 2 for reference). Nevertheless, MDCT-P for the triage

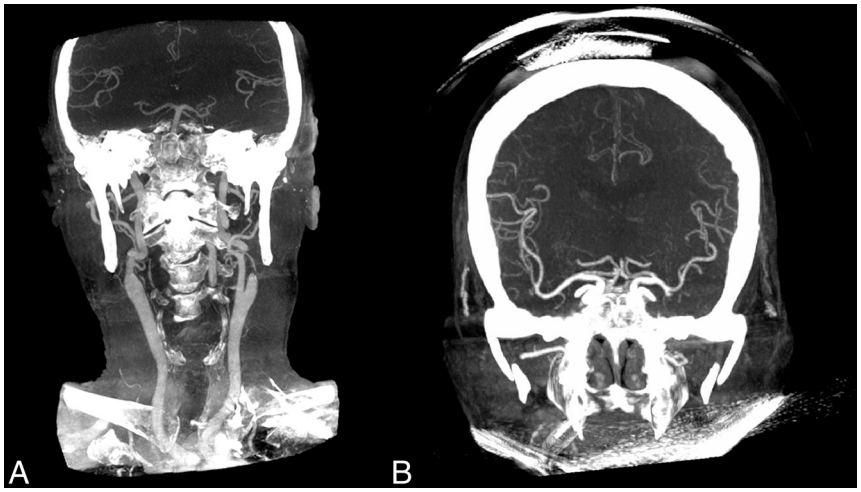

FIG 4. Comparison of the coverage area of portrait FDCT-A (*A*) and landscape FDCT-A (*B*) (based on reconstructed coronal MIPs).

of patients with late-window stroke has been validated in 2 randomized controlled trials,[11,12] while the technical equivalence of FDCT perfusion has yet to be established. A recent pilot trial of 13 patients showed promising results with high correlation for both ischemic core volume measurements on FDCT-P and MDCT-P and for follow-up infarct volumes.[4] We presuppose that our current results will contribute to the effort to reproduce such clinically meaningful results in larger patient collectives.

While it is widely accepted that FDCT offers higher spatial resolution for high-contrast structures (eg, vessels and bones), an essential shortcoming of FDCT-A is the limited z-coverage area.[13] This problem is largely solved by the development of a portrait FDCT-A protocol, which has a z-coverage area large enough to simultaneously visualize the circle of Willis and the intra- and extracranial carotid arteries down to their origins (Fig 4). This information is vital for planning interventions because the aortic arch configuration can influence the optimal vascular access site (eg, radial versus femoral) and for determining which catheters should be used for navigation to the intracranial vessels.[14,15] Another difference between FDCT-A and MDCT-A is that the timing of the acquisition after the injection of the contrast media bolus is operator-dependent. In contrast to MDCT-A, in which an automated Hounsfield unit threshold trigger is typically used for the start of the scan (by placing an ROI in the ascending aorta), the scan start has to be executed manually in FDCT-A.[16] To address this difference, we developed a "bolus-watching" protocol in which DSA is used to monitor the visible influx of contrast media into the common carotid arteries (following a 10-second delay after intravenous contrast injection) to manually initiate the 3D angiography.[16] According to previous measurements, this protocol adds only a minor radiation dose.[6]

The overall dose for perfusion and angiography on FDCT is, at 3.79 mSv, only slightly higher (8%) compared with MDCT. This difference is well below the accuracy threshold for the effective dose for patient measurements and, therefore, could be neglected. Both protocols (perfusion and angiography) are often used, even in the early time window of thrombolysis because it is more commonly recognized that perfusion plays an important role in the detection of medium and distal vessel occlusions,[17,18] ie, as potential targets for mechanical thrombectomy.[19] Recent measurements have shown an effective dose of 2 mSv for noncontrast FDCT parenchymal imaging, which is comparable with that of MDCT.[20,21] Because the cumulative dose of commonly used protocols in one-stop management of acute ischemic stroke does not differ substantially from routine MDCT, we anticipate that our findings will mitigate dose considerations in the triage decisions of patients with AIS.

The lower dose to the lens of the eye from FDCT-P compared with MDCT-P is explained by the reduced range of rotation of the flat detector, which is between 200° and 220° for most protocols with the radiation source being, importantly, below the patient.[22] However, the eye lens doses for the perfusion protocols have to be interpreted with caution because we were not able to incline the head of the phantom. Flexing the head toward the chin, as is performed for MDCT-P at our institution, might reduce the direct irradiation of the lens and, therefore, might reduce the dose substantially.[23] With regard to the standard MDCT-A protocol, the effect of inclining the head should not have a relevant proportional impact due to the large z-coverage area. However, there is an alternative protocol (HeadAngio_Xcare; Siemens Healthineers AG) using an organ-based tube-current modulation. which can reduce the eye lens dose. In this protocol, the direct x-ray exposure to the eye lens is reduced by lowering the x-ray tube current for a certain range of projection angles when the eye lenses are facing toward the x-ray tube. This protocol was not evaluated in this article. Overall, the certainty for the magnitude of the reduction of the lens dose is low because we were not able to incorporate all influencing factors.

One major strength of our study is that we used an anthropomorphic phantom with an identical measurement setup for both systems. This feature allows a reproducible comparison between different x-ray imaging modalities, acquisition protocols, and studies. This approach is superior to other measurement approaches, such as simulations or CT dose index–based approaches because the modern C-arm devices typically use a 210° rotation compared with MDCT, which has a 360° rotation. In the case of FDCT, this difference leads to a nonuniform dose distribution with the peak dose occurring in the central plane, on the side of the phantom closest to the radiation source.[24] Furthermore, the larger z-coverage of FDCT compared with MDCT renders the traditional, weighted CT dose index approaches impractical.[22] Another strength of our study is that we measured analogous protocols on both systems, enabling us to directly compare the effective dose to the patient from modern stroke imaging protocols.

However, our study has some limitations as well. The ATOM phantom is constructed to represent a broad cohort of different patients. Therefore, the actual dose to a patient might differ from the dose measured with the ATOM phantom. Because the ICRP

103 does not define the distribution and number of measurement points within the phantom, the investigator typically chooses these parameters.[9] This situation can lead to differences in the estimated effective dose, depending on the number and position of measurement points within an anthropomorphic phantom. In addition, Roser et al[25] showed that the organ-equivalent dose values calculated from discrete measurements might underestimate the simulated organ dose that was calculated on the basis of a continuous dose distribution by up to 50%. In the clinical routine, variance to our phantom study could occur not only with the collimation of the x-ray field but also the with the ROI, through normal practitioner and patient differences. However, because these parameters can be largely standardized in stroke protocols and because the coverage areas of the FDCT were at least as large as on the MDCT, our collimated results should be generalizable to clinical routine.

CONCLUSIONS

The estimated effective dose to the patient for FDCT-P and FDCT-A protocols on a modern biplane angiography system does not deviate substantially from analogous MDCT protocols.

ACKNOWLEDGMENTS

The authors gratefully acknowledge the technical support and assistance with phantom experiments from Stepina Elizaveta, PhD, and Brehm Marcus, PhD, from Siemens Healthineers, Forchheim, Germany.

Disclosure forms provided by the authors are available with the full text and PDF of this article at www.ajnr.org.

REFERENCES

1. Psychogios MN, Maier IL, Tsogkas I, et al. **One-stop management of 230 consecutive acute stroke patients: report of procedural times and clinical outcome.** *J Clin Med* 2019;8:2185 CrossRef Medline
2. Brehm A, Tsogkas I, Ospel JM, et al. **Direct to angiography suite approaches for the triage of suspected acute stroke patients: a systematic review and meta-analysis.** *Ther Adv Neurol Disord* 2022;15:17562864221078177 CrossRef Medline
3. Requena M, Olivé-Gadea M, Muchada M, et al. **Direct to angiography suite without stopping for computed tomography imaging for patients with acute stroke: a randomized clinical trial.** *JAMA Neurol* 2021;78:1099–1107 CrossRef Medline
4. Quispe-Orozco D, Farooqui M, Zevallos C, et al. **Angiography suite cone-beam computed tomography perfusion imaging in large-vessel occlusion patients using RAPID software: a pilot study.** *Stroke* 2021;52:e542–44 CrossRef Medline
5. Roser P, Birkhold A, Zhong X, et al. **Pitfalls in interventional x-ray organ dose assessment-combined experimental and computational phantom study: application to prostatic artery embolization.** *Int J Comput Assist Radiol Surg* 2019;14:1859–69 CrossRef Medline
6. Brehm A, Stamm G, Lüpke M, et al. **Effective dose to patient measurements for flat-detector computed tomography protocols in acute stroke care.** *Eur Radiol* 2020;30:5082–88 CrossRef Medline
7. Moore R, Waheed A, Burns B. *Rule of Nines*. StatPearls Publishing; 2021
8. **Basic anatomical and physiological data for use in radiological protection: reference values: a report of age- and gender-related differences in the anatomical and physiological characteristics of reference individuals—ICRP publication 89.** *Ann ICRP* 2002;32:5–265 Medline
9. **The 2007 Recommendations of the International Commission on Radiological Protection. ICRP Publication 103.** *Ann ICRP* 2007;37:1–332 CrossRef Medline
10. Struffert T, Deuerling-Zheng Y, Kloska S, et al. **Dynamic angiography and perfusion imaging using flat detector CT in the angiography suite: a pilot study in patients with acute middle cerebral artery occlusions.** *AJNR Am J Neuroradiol* 2015;36:1964–70 CrossRef Medline
11. Nogueira RG, Jadhav AP, Haussen DC, et al. **Thrombectomy 6 to 24 hours after stroke with a mismatch between deficit and infarct.** *N Engl J Med* 2018;378:11–21 CrossRef Medline
12. Albers GW, Marks MP, Kemp S, et al. **Thrombectomy for stroke at 6 to 16 hours with selection by perfusion imaging.** *N Engl J Med* 2018;378:708–18 CrossRef Medline
13. Struffert T, Hauer M, Banckwitz R, et al. **Effective dose to patient measurements in flat-detector and multislice computed tomography: a comparison of applications in neuroradiology.** *Eur Radiol* 2014;24:1257–65 CrossRef Medline
14. Chen SH, Snelling BM, Sur S, et al. **Transradial versus transfemoral access for anterior circulation mechanical thrombectomy: comparison of technical and clinical outcomes.** *J Neurointerv Surg* 2019;11:874–78 CrossRef Medline
15. McTaggart RA, Ospel JM, Psychogios MN, et al. **Optimization of endovascular therapy in the neuroangiography suite to achieve fast and complete (Expanded Treatment in Cerebral Ischemia 2c-3) reperfusion.** *Stroke* 2020;51:1961–68 CrossRef Medline
16. Psychogios MN, Behme D, Schregel K, et al. **One-stop management of acute stroke patients: minimizing door-to-reperfusion times.** *Stroke* 2017;48:3152–55 CrossRef Medline
17. Amukotuwa SA, Wu A, Zhou K, et al. **Time-to-maximum of the tissue residue function improves diagnostic performance for detecting distal vessel occlusions on CT angiography.** *AJNR Am J Neuroradiol* 2021;42:65–72 CrossRef Medline
18. Amukotuwa SA, Wu A, Zhou K, et al. **Distal medium vessel occlusions can be accurately and rapidly detected using Tmax maps.** *Stroke* 2021;52:3308–17 CrossRef Medline
19. Saver JL, Chapot R, Agid R, et al; Distal Thrombectomy Summit Group. **Thrombectomy for distal, medium vessel occlusions: a consensus statement on present knowledge and promising directions.** *Stroke* 2020;51:2872–84 CrossRef Medline
20. Lin HC, Lai TJ, Tseng HC, et al. **Radiation doses with various body weights of phantoms in brain 128-slice MDCT examination.** *J Radiat Res* 2019;60:466–75 CrossRef Medline
21. Petroulia VD, Kaesmacher J, Piechowiak EI, et al. **Evaluation of Sine Spin flat detector CT imaging compared with multidetector CT.** *J Neurointerv Surg* 2022 Mar 22 [Epub ahead of print] CrossRef Medline
22. Kalender WA, Kyriakou Y. **Flat-detector computed tomography (FD-CT).** *Eur Radiol* 2007;17:2767–79 CrossRef Medline
23. Nikupaavo U, Kaasalainen T, Reijonen V, et al. **Lens dose in routine head CT: comparison of different optimization methods with anthropomorphic phantoms.** *AJR Am J Roentgenol* 2015;204:117–23 CrossRef Medline
24. Fahrig R, Dixon R, Payne T, et al. **Dose and image quality for a cone-beam C-arm CT system.** *Med Phys* 2006;33:4541–50 CrossRef Medline
25. Roser P, Birkhold A, Preuhs A, et al. **XDose: toward online cross-validation of experimental and computational X-ray dose estimation.** *Int J Comput Assist Radiology Surg* 2021;16:1–10 CrossRef Medline